Structure and Motion Estimation from Apparent Contours under Circular Motion

Kwan-Yee K. Wong [a,*], Paulo R. S. Mendonça [b,1], Roberto Cipolla [b]

[a]*Department of Computer Science and Information Systems, The University of Hong Kong, Pokfulam Road, Hong Kong*

[b]*Department of Engineering, University of Cambridge, Cambridge, CB2 1PZ, UK*

Abstract

In this paper we address the problem of recovering structure and motion from the apparent contours of a smooth surface. Fixed image features under circular motion and their relationships with the intrinsic parameters of the camera are exploited to provide a simple parameterization of the fundamental matrix relating any pair of views in the sequence. Such a parameterization allows a trivial initialization of the motion parameters, which all bear physical meanings. It also greatly reduces the dimension of the search space for the optimization problem, which can now be solved using only 2 epipolar tangents. In contrast to previous methods, the motion estimation algorithm introduced here can cope with incomplete circular motion and more widely spaced images. Existing techniques for model reconstruction from apparent contours are then reviewed and compared. Experiment on real data has been carried out and the 3D model reconstructed from the estimated motion is presented.

Key words: structure and motion, circular motion, apparent contours.

1 Introduction

The recovery of structure and motion from sequences of images is a central problem in computer vision, and the search for its solution has generated a rich pool of algorithms [1–4]. Most of these algorithms rely on correspondences of points or lines

---

* Corresponding author.
  Email addresses: `kykwong@csis.hku.hk` (Kwan-Yee K. Wong),
`prdsm2@eng.cam.ac.uk` (Paulo R. S. Mendonça), `cipolla@eng.cam.ac.uk`
(Roberto Cipolla).

between images [5,6], and work well when the scene being viewed is composed of polyhedral parts. However, for smooth surfaces without noticeable texture, point and line correspondences may not be easily established. In this case the *apparent contour* [7] of the surface is very often the only feature available, and is certainly the most important one. This calls for the development of a completely different set of techniques, as the ones found in [8–11,7,12,13].

In this paper we address the problem of structure and motion recovery from the apparent contours of smooth surfaces. Section 2 first briefly reviews the concepts of *contour generators* [7] and apparent contours in viewing smooth surfaces under perspective projection. The problem of estimating the motion parameters of turntable sequences is tackled in Section 3. Fixed image features under circular motion and their relationships with the intrinsic parameters of the camera are exploited to provide a simple parameterization of the fundamental matrix relating any pair of views in the sequence. This parameterization allows a trivial initialization of the motion parameters, which all bear physical meanings. It also greatly reduces the dimension of the search space for the optimization problem. By exploiting such a parameterization, a novel algorithm for circular motion estimation from apparent contours is introduced, which only requires the presence of 2 pairs of corresponding epipolar tangents. The algorithm introduced here can also cope with incomplete circular motion and more widely spaced images. Existing techniques for model reconstruction from apparent contours are then reviewed and compared in Section 4. Finally, experimental result on real data is presented in Section 5.

2 Contour Generators and Apparent Contours

Consider a point P on a smooth surface S. Under perspective projection the vector position $\mathbf{r}$ of P is given by

$$\mathbf{r} = \mathbf{c} + \lambda \mathbf{p}, \tag{1}$$

where $\mathbf{c}$ is the camera center, $\mathbf{p}$ is the unit viewing direction and λ is the depth of the point P along the viewing direction $\mathbf{p}$ from $\mathbf{c}$. For a given camera center $\mathbf{c}$, the set of points on the surface for which the visual ray is tangent to S is called the *contour generator* [14,7]. In the literature, the contour generator is also known as the *extremal boundary* [15] or the *rim* [8]. The contour generator separates the visible part from the occluded part of S, and can be parameterized by s as [7]

$$\mathbf{r}(s) = \mathbf{c} + \lambda(s)\mathbf{p}(s) \text{ such that} \tag{2}$$
$$\mathbf{p}(s) \cdot \mathbf{n}(s) = 0, \tag{3}$$

where $\mathbf{n}(s)$ is the unit surface normal of S at $\mathbf{r}(s)$. From equations (2) and (3), it is easy to see that the contour generator depends on both the viewpoint and the local surface geometry.

A contour generator is projected onto the image plane as an *apparent contour* (also known as a *profile* or *silhouette*). If the camera is fully calibrated, the viewing rays $\mathbf{p}(s)$ of the contour generator can be recovered from the apparent contour directly. These rays define a *viewing cone* on which the contour generator lies, and within which the object is confined (see Fig. 1). However, the depth parameter $\lambda(s)$ in equation (2), and hence the contour generator itself, cannot be determined from a single view alone. It is easy to show that, like the viewing ray, the tangent to the apparent contour also lies on the tangent plane of the surface at $\mathbf{r}(s)$. This allows the unit surface normal at $\mathbf{r}(s)$ to be determined up to a sign by [7]

$$\mathbf{n}(s) = \frac{\mathbf{p}(s) \times \frac{d\,\mathbf{p}(s)}{d\,s}}{\left|\mathbf{p}(s) \times \frac{d\,\mathbf{p}(s)}{d\,s}\right|}. \tag{4}$$

The sign of $\mathbf{n}(s)$ can be fixed if the side of the apparent contour on which the surface lies is known.
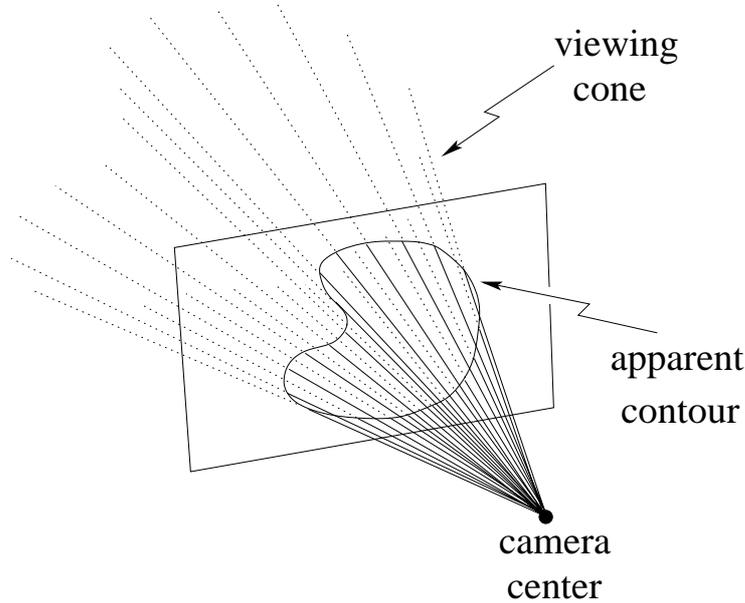

Fig. 1. The viewing rays of the contour generator can be recovered from the apparent contour and the camera center. These rays define a viewing cone on which the contour generator lies, and within which the object is confined.

3   Motion Estimation from Apparent Contours

The fundamental difficulty in estimating the motion of a smooth surface arises from the fact that contour contours are viewpoint dependent. Due to the viewpoint dependency of the contour generators, the apparent contours of a smooth surface observed from 2 distinct viewpoints will be, in general, the projections of 2 different space curves (contour generators). As a result, unlike point or line features, the apparent

contours do not readily provide image correspondences that allow for the computation of the *epipolar geometry* [16,17], summarized by the *fundamental matrix* [5]. This characteristic makes the motion estimation problem difficult even for humans under certain circumstances [18]. A possible solution to this is the use of *epipolar tangencies* [9,10,19], as shown in Fig. 2. An epipolar tangent point is the projection of a *frontier point* [20–22] (referred to as a *fixed point* in [9]), which is the intersection of 2 contour generators. Since the frontier points are fixed points in space that can be seen in both views, their images will provide point correspondences.
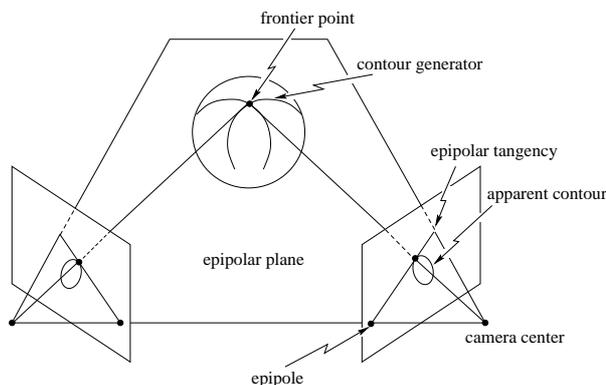

Fig. 2. A frontier point is the intersection of 2 contour generators and is visible in both views. The frontier point is projected onto a point in the apparent contour which is also an epipolar tangent point.

If enough epipolar tangencies are available, the epipolar geometry can be estimated and hence the motion can be determined up to a *projective transformation* [23,24]. The *intrinsic parameters* [17] of the cameras can then be used to reduce this ambiguity to a similarity transformation [25,26]. The major problem of such an approach [21,27] is that a minimum of 7 pairs of corresponding epipolar tangents is required, a number which seldom occurs in practical situations. By using an affine approximation [28–30], a similar technique that only requires 4 pairs of corresponding epipolar tangents was developed in [31], resulting in a simpler and more robust estimation of the epipolar geometry. Although more realistic, such a demand is still restrictive. By constraining the motion to be circular, a parameterization of the fundamental matrix with only 6 degrees of freedom is possible [32,4,33]. This parameterization explicitly takes into account the main image features of circular motion, namely the image of the rotation axis, the horizon and a special vanishing point, which are fixed throughout the sequence. This makes it possible to estimate the epipolar geometry by using only 2 epipolar tangents [33].

In [34], a practical algorithm has been introduced for the estimation of motion and structure from the apparent contours of a rotating object. The image of the rotation axis and the special vanishing point are first determined by estimating the harmonic homology associated with the image of the surface of revolution spanned by the rotating object. In order to obtain such an image, a dense image sequence from a complete circular motion is required. In this paper, the parameters of the harmonic

4

homology and other motion parameters are estimated simultaneously by minimizing the reprojection errors of the epipolar tangents. The algorithm presented here does not require the image of such a surface of revolution and can thus cope with incomplete circular motion and more widely spaced images, an advantage over the algorithm presented in [34].

3.1 Symmetry and Epipolar Geometry under Circular Motion

Consider a pin-hole camera rotating about a fixed axis, with its intrinsic parameters kept constant. The projection of the rotation axis will be a line $\mathbf{l}_s$ which is *pointwise fixed* on each image. This means that any point $\mathbf{x}$ along $\mathbf{l}_s$ must satisfy the equation $\mathbf{x}^T\mathbf{F}\mathbf{x} = 0$, where $\mathbf{F}$ is the fundamental matrix associated with any image pair in the sequence. Let Π_h be the plane that contains the trajectory of the camera center. The image of this plane is a special line $\mathbf{l}_h$ named the *horizon*, which is fixed throughout the sequence. In general, $\mathbf{l}_s$ and $\mathbf{l}_h$ are not orthogonal. By definition, the epipoles are the projections of the camera center and must therefore lie on $\mathbf{l}_h$. Another fixed feature is the vanishing point $\mathbf{v}_x$, which corresponds to the normal direction $\mathbf{N}_x$ of the plane Π_s defined by the camera center and the axis of rotation. Since $\mathbf{N}_x$ is parallel to the plane Π_h, it follows that $\mathbf{v}_x$ also lies on $\mathbf{l}_h$ (i.e. $\mathbf{v}_x^T\mathbf{l}_h = 0$). A detailed discussion of the above can be found in [32,4,33].

Consider now a pair of images taken from the circular motion sequence, and let $\mathbf{F}$ be the fundamental matrix associated with this pair. It has been shown that corresponding epipolar lines associated with $\mathbf{F}$ are related to each other by a harmonic homology $\mathbf{W}$ [33], given by

$$\mathbf{W} = \mathbb{I} - 2\frac{\mathbf{v}_x\mathbf{l}_s^T}{\mathbf{v}_x^T\mathbf{l}_s}. \tag{5}$$

Note that $\mathbf{W}$ has 4 degrees of freedom: 2 corresponding to the axis and 2 corresponding to the vanishing point. If the rotating camera points directly towards the axis of rotation, $\mathbf{v}_x$ will be at infinity and $\mathbf{W}$ will be reduced to a skew symmetry with only 3 degrees of freedom. Besides, if the camera also has zero skew and aspect ratio 1, the transformation will be further specialized to a bilateral symmetry with only 2 degrees of freedom. A pictorial description of these transformations can be seen in Fig. 3.

In [35], an algorithm has been presented for estimating the camera intrinsic parameters from 2 or more apparent contours of surfaces of revolution. For each apparent contour, the associated harmonic homology $\mathbf{W}$ is estimated and this provides 2 constraints on the camera intrinsic parameters:

$$\mathbf{v}_x = \mathbf{K}\mathbf{K}^T\mathbf{l}_s, \tag{6}$$

where $\mathbf{K}$ is the 3×3 camera calibration matrix. Conversely, if the camera intrinsic
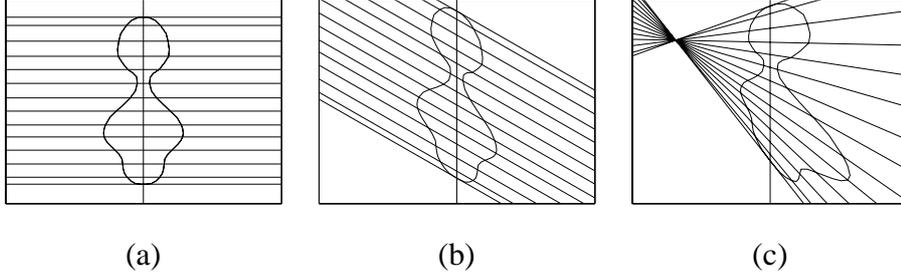
(a)   (b)   (c)

Fig. 3. (a) A curve displaying bilateral symmetry. The horizon is orthogonal to the axis. (b) Same curve, distorted by an affine transformation. The horizon is no longer orthogonal to the axis, and each side of the curve is mapped to the other by a skew symmetry transformation. (c) The curve is now distorted by a special projective transformation (harmonic homology), and the lines of symmetry intersect at a point corresponding to the vanishing point.

parameters are known, equation (6) provides 2 constraints on $\mathbf{W}$ and $\mathbf{W}$ will then have only 2 degrees of freedom.

3.2   Parameterizations of the Fundamental Matrix

In [5,36], it has been shown that any fundamental matrix $\mathbf{F}$ can be parameterized as $\mathbf{F} = [\mathbf{e}_2]_\times \mathbf{M}$, where $\mathbf{M}^{-\mathrm{T}}$ is any matrix that maps corresponding epipolar lines from one image to the other, and $\mathbf{e}_2$ is the epipole in the second image. In the case of circular motion, it follows that

$$\mathbf{F} = [\mathbf{e}_2]_\times \mathbf{W}. \tag{7}$$

Note that $\mathbf{F}$ has 6 degrees of freedom: 2 to fix $\mathbf{e}_2$, and 4 to determine $\mathbf{W}$. It follows from (6) that if the camera intrinsic parameters are known, 2 parameters are enough to define $\mathbf{W}$ and thus $\mathbf{F}$ will have only 4 degrees of freedom.

An alternative parameterization for the fundamental matrix in the case of circular motion is given by [32,4,33]

$$\mathbf{F} = [\mathbf{v}_x]_\times + \kappa \tan \frac{\theta}{2}(\mathbf{l}_\mathrm{s}\mathbf{l}_\mathrm{h}^\mathrm{T} + \mathbf{l}_\mathrm{h}\mathbf{l}_\mathrm{s}^\mathrm{T}), \tag{8}$$

where θ is the angle of rotation, and κ is a constant which can be determined from the determinant of the camera calibration matrix if $\mathbf{l}_\mathrm{s}$, $\mathbf{v}_x$ and $\mathbf{l}_\mathrm{h}$ are properly normalized [33]. θ is the only parameter which depends on the particular pair of images being considered, while the other 4 terms are common to all pairs of images in the sequence. When the camera calibration matrix is known, 2 parameters are enough to fix $\mathbf{l}_\mathrm{s}$ and $\mathbf{v}_x$. Since $\mathbf{v}_x$ must lie on $\mathbf{l}_\mathrm{h}$, only 1 further parameter is needed to fix $\mathbf{l}_\mathrm{h}$. As a result, the fundamental matrix has only 4 degrees of freedom.

6

By exploiting the parameterization given in (8), the $\binom{N}{2} = \frac{N(N-1)}{2}$ fundamental matrices relating all possible image pairs in a sequence of N images, taken by a rotating camera with known intrinsic parameters, can be defined with the 3 parameters that fix $\mathbf{l}_s$, $\mathbf{v}_x$ and $\mathbf{l}_h$, together with the $N-1$ angles of rotation between adjacent cameras. By enforcing the epipolar constraint on the corresponding epipolar tangent points, these $N+2$ motion parameters can be estimated by minimizing the reprojection errors of corresponding epipolar tangents. Given a pair of views, the associated fundamental matrix $\mathbf{F}$ is formed from the current estimate of the motion parameters, and the epipoles $\mathbf{e}$ and $\mathbf{e}'$ are obtained from the right and left nullspaces of $\mathbf{F}$ respectively (see Fig. 4). The epipolar tangent points $\mathbf{t}$ and $\mathbf{t}'$ are located and the reprojection errors are then given by the geometric distances between the epipolar tangent points and their epipolar lines [5]

$$\delta = \frac{\mathbf{t}'^{\mathrm{T}}\mathbf{F}\mathbf{t}}{\sqrt{(\mathbf{F}^{\mathrm{T}}\mathbf{t}')_1^2 + (\mathbf{F}^{\mathrm{T}}\mathbf{t}')_2^2}}, \text{ and} \tag{9}$$

$$\delta' = \frac{\mathbf{t}'^{\mathrm{T}}\mathbf{F}\mathbf{t}}{\sqrt{(\mathbf{F}\mathbf{t})_1^2 + (\mathbf{F}\mathbf{t})_2^2}}, \tag{10}$$

where $(\mathbf{F}^{\mathrm{T}}\mathbf{t}')_1$ and $(\mathbf{F}^{\mathrm{T}}\mathbf{t}')_2$ indicate the 1st and 2nd coefficients of $\mathbf{F}^{\mathrm{T}}\mathbf{t}'$ respectively. Similarly, $(\mathbf{F}\mathbf{t})_1$ and $(\mathbf{F}\mathbf{t})_2$ indicate the 1st and 2nd coefficients of $\mathbf{F}\mathbf{t}$ respectively. By exploiting the 2 epipolar tangents at the top and bottom of the apparent contours, there will be totally $2\binom{N}{2} = N(N-1)$ measurements from all pairs of images. Due to the dependency between the associated fundamental matrices, however, these $N(N-1)$ measurements only provide $2N$ (or 2 when $N=2$) independent constraints on the $N+2$ parameters. As a result, a solution will be possible when $N \geq 3$.

The minimization of the reprojection errors will generate a consistent set of fundamental matrices, which, together with the camera intrinsic parameters, can be decomposed into a set of camera matrices describing a circular motion compatible with the image sequence. The algorithm for motion estimation is summarized in Algorithm 1.

4   Model Reconstruction from Apparent Contours

Depending on the nature of the surface and the image sequence, either a surface model or a volumetric model can be constructed from the set of apparent contours with known (or estimated) viewer motion. If a dense, continuous sequence is
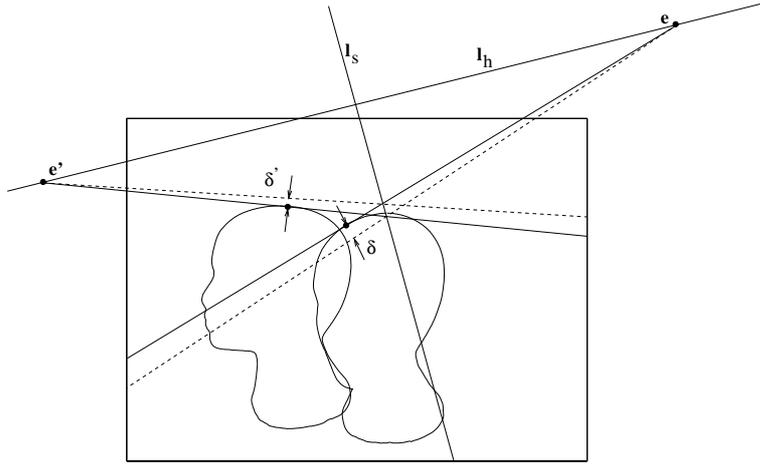
Fig. 4. The parameters of the fundamental matrix associated with each pair of images in the sequence can be estimated by minimizing the reprojection errors of the epipolar tangents. The solid lines are tangents to the apparent contours passing through the corresponding epipoles, and the dash lines are the epipolar lines corresponding to the tangent points.

Algorithm 1 Motion Estimation from Apparent Contours.

   extract the apparent contours of the rotating object
    using cubic B-spline snakes;
   initialize $\mathbf{l}_s$, $\mathbf{l}_h$ and the $N-1$ angles between the N cameras;
   while not converged **do**
     for each image in the sequence **do**
      form the fundamental matrices with the next 2 images;
      locate epipolar tangents;
      compute reprojection errors of the epipolar tangents;
     end for
     update parameters to minimize the rms reprojection errors
      using the conjugate gradient method [37];
   end while

---

available, a surface model can be obtained by reconstructing the contour generators of a simple surface using differential techniques [7,11–13]. On the other hand, if only sparse, discrete views are available and the object has relatively complex topologies, volume intersection techniques [38,39] can be employed to produce a volumetric model which represents the visual hull [40,41] of the object. A brief review and comparison of existing approaches for model reconstruction from apparent contours are given in the following subsections.

4.1 Surface Approach

The surface reconstruction of smooth objects from apparent contours was pioneered by Giblin and Weiss [42]. Under the assumption of orthographic projection, they

demonstrated that a surface can be reconstructed from the envelope of all its tangent planes computed directly from the family of apparent contours of the surface under planar viewer motion.

In [7], Cipolla and Blake extended the studies of Giblin and Weiss to curvilinear viewer motion under perspective projection, and developed the *osculating circle method* by introducing the *epipolar parameterization*. Given 3 corresponding points under the epipolar parameterization in 3 consecutive apparent contours, the viewing rays defined by them are projected onto the epipolar plane defined by the first two. By assuming that the curvature of the *epipolar curve* is locally constant, the epipolar curve can be approximated as part of a circle tangent to these (projected) viewing rays. In [11], Vaillant and Faugeras developed a technique similar to that presented in [7], except that the surface is parameterized by the *radial curves* instead of the epipolar curves. Based on the osculating circle method, Szeliski and Weiss [13] used a linear smoother to compute epipolar curves on the whole surface together with an estimate of uncertainty, and reported improvements in the reconstruction. The osculating circle methods require the camera motion to be close to linear and the surface remains on the same side of the tangents in the projection plane.

In [12], Boyer and Berger derived a depth formulation from a local approximation of the surface up to order two for discrete motion. Their technique allows the local shape to be estimated from 3 consecutive contours by solving a pair of simultaneous equations, and it only requires that the surfaces are at least C^2 and are not locally planar. In [43], Wong et al. developed a simple triangulation technique based on a finite-difference implementation of [7]. Despite its simplicity, the method developed in [43] was reported to produce results comparable to those in [7] and [12].

4.2 Volumetric Approach

The volume intersection technique for constructing volumetric descriptions of objects from multiple views was first proposed by Martin and Aggarwal [44], who introduced the *volume segment* representation. In [45], Chien and Aggarwal presented an algorithm for generating an octree [46,47] of an object from 3 orthogonal views under orthographic projection. Their work was further developed by Ahuja and Veenstra [48], who extended the algorithm to handle images from any subset of 13 standard viewing directions.

In [49], Hong and Shneier introduced a technique for generating an octree from multiple arbitrary views under perspective projection. Their approach first constructs an octree for each image by projecting the octree cubes onto the image and intersecting their projections with the apparent contour, and the final octree of the object is given by the intersection of the octrees obtained from all images. In

[38], Potmesil described a similar approach in which the images are represented by *quadtrees* to facilitate the intersection of the projections of the cubes with the apparent contours.

Other similar approaches also include [50] and [51], where the octree for each image is constructed by intersecting, in 3D space, the octree cubes with the polyhedral cone formed from the back-projection of the apparent contours. In [39], Szeliski introduced an efficient algorithm which constructs an octree in a hierarchical coarse-to-fine fashion. His approach is similar to that of [38], except that only a single octree is constructed using all the images simultaneously.

Despite its modeling power, an octree representation is not very suitable for high speed rendering. Based on [39], Fitzgibbon et al. [4] implemented a technique in which the standard *marching cubes algorithm* [52] is applied to extract surface triangle patches from the octree. The resulting surface model can then be displayed efficiently with conventional graphics rendering algorithms. In [53], Sullivan and Ponce presented an algorithm in which a G^1-continuous spline surface is first constructed from the polyhedral approximation of the object obtained by intersecting the viewing cones associated with the apparent contours. Such a spline surface is then deformed to minimize the true distance to the rays bounding those viewing cones.

5   Experiments and Results

The experimental sequence consisted of 18 images of a polystyrene head model taken under controlled circular motion (see Fig. 5). Each image was taken after rotating the model by $20°$ on a hand-operated turntable with a resolution of $0.01°$. The intrinsic parameters of the camera were obtained by an offline calibration process [54,17] using a calibration grid.

The motion was estimated using the algorithm described in Section 3.3. The image of the rotation axis l_s and the horizon l_h were initialized manually, and the rotation angles were all initialized to an arbitrary angle. The rms reprojection error was minimized using the *conjugate gradient method* [37], with the gradient vector computed by finite differences using a delta change of 10^{-6} for each parameter. Note that neither the knowledge of the rotation angles nor the fact that it was a closed sequence was used in estimating the motion.

The initial and final configurations of the image of the rotation axis and the horizon are shown in Fig. 6, and the estimated rotation angles between adjacent images and their errors are shown in Table 1. It can be seen from Table 1 that the errors in the rotation angles ranged from $0.0077°$ to $0.4001°$, and the rms error of the rotation angles was only $0.2131°$. The resulting camera poses are shown in Fig. 7. The 3D

model built from the estimated motion, using the technique presented by Fitzgibbon et al. in [4], is shown in Fig. 8.

Fig. 5. Eighteen images of a polystyrene head model under controlled circular motion. Each image was taken after rotating the model by $20°$ on a turntable with a resolution of $0.01°$.

6 Conclusions

The novel algorithm for circular motion estimation from apparent contours introduced here has a main advantage over previously proposed methods, in that it only requires the presence of 2 pairs of corresponding epipolar tangents. In [34] we have developed a robust technique to tackle the same problem with trivial initializations, but it can only be applied when the image of the surface of revolution swept out by the rotating object can be obtained. The algorithm presented here overcomes this limitation, and can be used when as few as 3 images of the rotating object are available. The method introduced in this paper is robust and accurate. Experiment on real data has produced convincing 3D model, demonstrating the validity of the technique proposed.
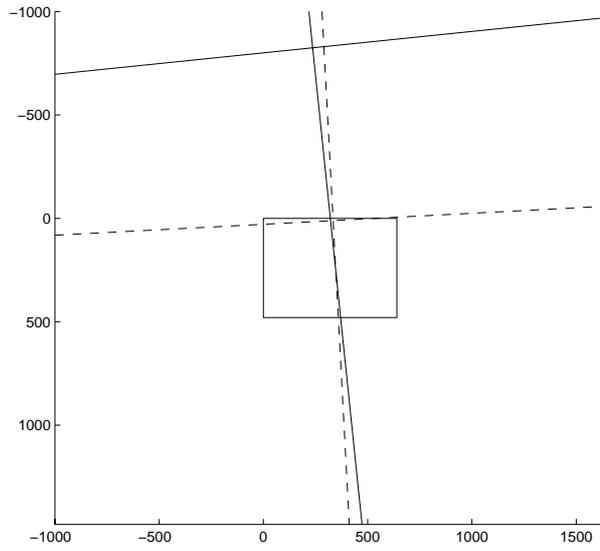
11

Fig. 6. The initial (in dash lines) and final (in solid lines) configurations of the image of the rotation axis l_s and the horizon l_h.

Table 1
Estimated rotation angles between adjacent images.

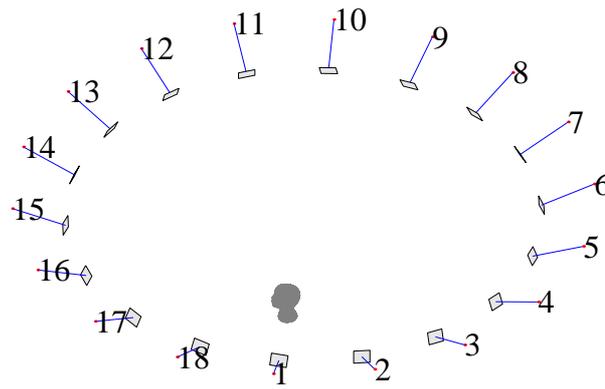| views	rotation angle	error	views	rotation angle	error
1–2	19.8856°	−0.1144°	10–11	20.1026°	+0.1026°
2–3	19.9660°	−0.0340°	11–12	20.0241°	+0.0241°
3–4	20.3055°	+0.3055°	12–13	20.1651°	+0.1651°
4–5	19.9707°	−0.0293°	13–14	20.2053°	+0.2053°
5–6	20.0224°	+0.0224°	14–15	20.1401°	+0.1401°
6–7	19.8686°	−0.1314°	15–16	20.3132°	+0.3132°
7–8	20.3860°	+0.3860°	16–17	20.0292°	+0.0292°
8–9	20.3708°	+0.3708°	17–18	19.5999°	−0.4001°
9–10	19.9923°	−0.0077°			

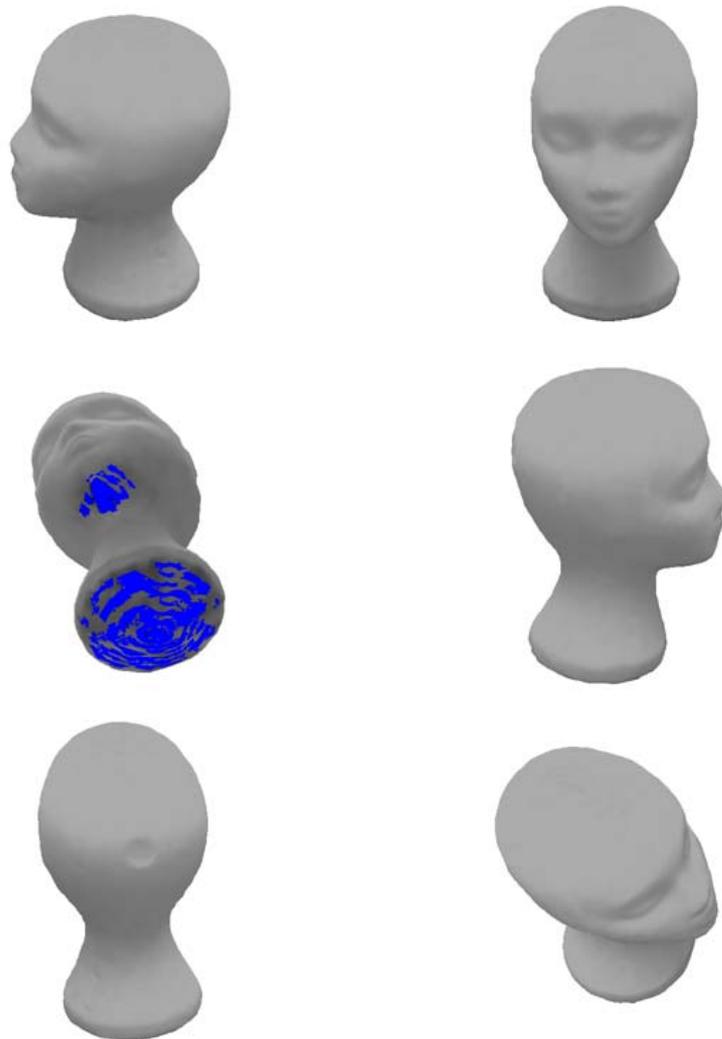Fig. 7. Camera poses estimated from the polystyrene head sequence.

Fig. 8. 3D model of the polystyrene head built from the estimated circular motion.

References

[1] C. Tomasi, T. Kanade, Shape and motion from image streams under orthography: A factorization method, Int. Journal of Computer Vision 9 (2) (1992) 137–154.

[2] P. A. Beardsley, A. Zisserman, D. W. Murray, Sequential updating of projective and affine structure from motion, Int. Journal of Computer Vision 23 (3) (1997) 235–259.

[3] R. Koch, M. Pollefeys, L. van Gool, Multi viewpoint stereo from uncalibrated video sequences, in: H. Burkhardt, B. Neumann (Eds.), Proc. 5th European Conf. on Computer Vision, Vol. 1406 of Lecture Notes in Computer Science, Springer–Verlag, Freiburg, Germany, 1998, pp. 55–71.

[4] A. W. Fitzgibbon, G. Cross, A. Zisserman, Automatic 3D model construction for turn-table sequences, in: R. Koch, L. Van Gool (Eds.), 3D Structure from Multiple Images of Large-Scale Environments, European Workshop SMILE'98, Vol. 1506 of Lecture Notes in Computer Science, Springer–Verlag, Freiburg, Germany, 1998, pp. 155–170.

[5] Q. T. Luong, O. D. Faugeras, The fundamental matrix: Theory, algorithm, and stability analysis, Int. Journal of Computer Vision 17 (1) (1996) 43–75.

[6] R. Hartley, Lines and points in three views and the trifocal tensor, Int. Journal of Computer Vision 22 (2) (1997) 125–140.

[7] R. Cipolla, A. Blake, Surface shape from the deformation of apparent contours, Int. Journal of Computer Vision 9 (2) (1992) 83–112.

[8] J. J. Koenderink, What does the occluding contour tell us about solid shape?, Perception 13 (1984) 321–330.

[9] J. H. Rieger, Three dimensional motion from fixed points of a deforming profile curve, Optics Letters 11 (3) (1986) 123–125.

[10] J. Porrill, S. B. Pollard, Curve matching and stereo calibration, Image and Vision Computing 9 (1) (1991) 45–50.

[11] R. Vaillant, O. D. Faugeras, Using extremal boundaries for 3D object modeling, IEEE Trans. on Pattern Analysis and Machine Intelligence 14 (2) (1992) 157–173.

[12] E. Boyer, M. O. Berger, 3d surface reconstruction using occluding contours, Int. Journal of Computer Vision 22 (3) (1997) 219–233.

[13] R. Szeliski, R. Weiss, Robust shape recovery from occluding contours using a linear smoother, Int. Journal of Computer Vision 28 (1) (1998) 27–44.

[14] D. Marr, Analysis of occluding contour, Proc. Royal Soc. London B 197 (1977) 441–475.

[15] H. G. Barrow, J. M. Tenenbaum, Recovering intrinsic scene characteristics from images, in: A. R. Hanson, E. M. Riseman (Eds.), Computer Vision Systems, Academic Press, New York, 1978, pp. 3–26.

[16] H. H. Baker, T. O. Binford, Depth from edge and intensity based stereo, in: Proc. 7th Int. Joint Conf. on Artificial Intelligence, Vancouver, BC, Canada, 1981, pp. 631–636.

[17] O. D. Faugeras, Three-Dimensional Computer Vision: a Geometric Viewpoint, MIT Press, Cambridge, MA, 1993.

[18] F. E. Pollick, Perceiving shape from profiles, Perception and Psychophysics 55 (2) (1994) 152–161.

[19] R. Cipolla, The visual motion of curves and surfaces, Phil. Trans. Royal Soc. London A 356 (1998) 1103–1121.

[20] P. J. Giblin, F. E. Pollick, J. E. Rycroft, Recovery of an unknown axis of rotation from the profiles of a rotating surface, Journal of Optical Soc. of America A 11 (7) (1994) 1976–1984.

[21] R. Cipolla, K. E. Åström, P. J. Giblin, Motion from the frontier of curved surfaces, in: Proc. 5th Int. Conf. on Computer Vision, Cambridge, MA, USA, 1995, pp. 269–275.

[22] R. Cipolla, P. J. Giblin, Visual Motion of Curves and Surfaces, Cambridge University Press, Cambridge, UK, 1999.

[23] O. D. Faugeras, What can be seen in three dimensions with an uncalibrated stereo rig, in: G. Sandini (Ed.), Proc. 2nd European Conf. on Computer Vision, Vol. 588 of Lecture Notes in Computer Science, Springer–Verlag, Santa Margherita Ligure, Italy, 1992, pp. 563–578.

[24] R. I. Hartley, Estimation of relative camera positions for uncalibrated cameras, in: G. Sandini (Ed.), Proc. 2nd European Conf. on Computer Vision, Vol. 588 of Lecture Notes in Computer Science, Springer–Verlag, Santa Margherita Ligure, Italy, 1992, pp. 579–587.

[25] H. C. Longuet-Higgins, A computer algorithm for reconstructing a scene from two projections, Nature 293 (1981) 133–135.

[26] O. Faugeras, Stratification of three-dimensional vision: Projective, affine and metric representations, Journal of Optical Soc. of America A 12 (3) (1995) 465–484.

[27] K. Åström, R. Cipolla, P. Giblin, Generalised epipolar constraints, Int. Journal of Computer Vision 33 (1) (1999) 51–72.

[28] J. L. Mundy, A. Zisserman, Geometric Invariance in Computer Vision, MIT Press, Cambridge, MA, 1992.

[29] L. S. Shapiro, A. Zisserman, M. Brady, 3D motion recovery via affine epipolar geometry, Int. Journal of Computer Vision 16 (2) (1995) 147–182.

[30] L. Quan, Self-calibration of an affine camera from multiple views, Int. Journal of Computer Vision 19 (1) (1996) 93–105.

[31] P. R. S. Mendonça, R. Cipolla, Estimation of epipolar geometry from apparent contours: Affine and circular motion cases, in: Proc. Conf. Computer Vision and Pattern Recognition, Vol. I, Fort Collins, CO, 1999, pp. 9–14.

[32] T. Vieville, D. Lingrand, Using singular displacements for uncalibrated monocular visual systems, in: B. Buxton, R. Cipolla (Eds.), Proc. 4th European Conf. on Computer Vision, Vol. 1065 of Lecture Notes in Computer Science, Springer–Verlag, Cambridge, UK, 1996, pp. 207–216.

[33] P. R. S. Mendonça, K.-Y. K. Wong, R. Cipolla, Recovery of circular motion from profiles of surfaces, in: B. Triggs, A. Zisserman, R. Szeliski (Eds.), Vision Algorithms: Theory and Practice, Vol. 1883 of Lecture Notes in Computer Science, Springer–Verlag, Corfu, Greece, 1999, pp. 151–167.

[34] P. R. S. Mendonça, K.-Y. K. Wong, R. Cipolla, Epipolar geometry from profiles under circular motion, IEEE Trans. on Pattern Analysis and Machine Intelligence 23 (6) (2001) 604–616.

[35] K.-Y. K. Wong, P. R. S. Mendonça, R. Cipolla, Camera calibration from symmetry, in: R. Cipolla, R. Martin (Eds.), The Mathematics of Surfaces IX, Springer–Verlag, Cambridge, UK, 2000, pp. 214–226.

[36] Z. Zhang, Determining the epipolar geometry and its uncertainty: A review, Int. Journal of Computer Vision 27 (2) (1998) 161–195.

[37] W. H. Press, S. A. Teukolsky, W. T. Vetterling, B. P. Flannery, Numerical Recipes in C : The Art of Scientific Computing, 2nd Edition, Cambridge University Press, Cambridge, UK, 1993.

[38] M. Potmesil, Generating octree models of 3D objects from their silhouettes in a sequence of images, Computer Vision, Graphics and Image Processing 40 (1) (1987) 1–29.

[39] R. Szeliski, Rapid octree construction from image sequences, Computer Vision, Graphics and Image Processing 58 (1) (1993) 23–32.

[40] A. Laurentini, The visual hull concept for silhouette-based image understanding, IEEE Trans. on Pattern Analysis and Machine Intelligence 16 (2) (1994) 150–162.

[41] A. Laurentini, How far 3D shapes can be understood from 2D silhouettes, IEEE Trans. on Pattern Analysis and Machine Intelligence 17 (2) (1995) 188–195.

[42] P. J. Giblin, R. S. Weiss, Reconstructions of surfaces from profiles, in: Proc. 1st Int. Conf. on Computer Vision, London, UK, 1987, pp. 136–144.

[43] K.-Y. K. Wong, P. R. S. Mendonça, R. Cipolla, Reconstruction and motion estimation from apparent contours under circular motion, in: T. Pridmore, D. Elliman (Eds.), Proc. British Machine Vision Conference, Vol. 1, Nottingham, UK, 1999, pp. 83–92.

[44] W. N. Martin, J. K. Aggarwal, Volumetric descriptions of objects from multiple views, IEEE Trans. on Pattern Analysis and Machine Intelligence 5 (2) (1983) 150–158.

[45] C. H. Chien, J. K. Aggarwal, Volume/surface octrees for the representation of three-dimensional objects, Computer Vision, Graphics and Image Processing 36 (1) (1986) 100–113.

[46] C. L. Jackins, S. L. Tanimoto, Oct-trees and their use in representing three-dimensional objects, Computer Graphics Image Processing 14 (3) (1980) 249–270.

[47] D. J. Meagher, Geometric modeling using octree encoding, Computer Graphics Image Processing 19 (2) (1982) 129–147.

[48] N. Ahuja, J. Veenstra, Generating octrees from object silhouettes in orthographic views, IEEE Trans. on Pattern Analysis and Machine Intelligence 11 (2) (1989) 137–149.

[49] T. H. Hong, M. O. Shneier, Describing a robot's workspace using a sequence of views from a moving camera, IEEE Trans. on Pattern Analysis and Machine Intelligence 7 (6) (1985) 721–726.

[50] H. Noborio, S. Fukuda, S. Arimoto, Construction of the octree approximating three-dimensional objects by using multiple views, IEEE Trans. on Pattern Analysis and Machine Intelligence 10 (6) (1988) 769–782.

[51] S. K. Srivastava, N. Ahuja, Octree generation from object silhouettes in perspective views, Computer Vision, Graphics and Image Processing 49 (1) (1990) 68–84.

[52] W. E. Lorensen, H. E. Cline, Marching cubes: a high resolution 3D surface construction algorithm, ACM Computer Graphics 21 (4) (1987) 163–169.

[53] S. Sullivan, J. Ponce, Automatic model construction and pose estimation from photographs using triangular splines, IEEE Trans. on Pattern Analysis and Machine Intelligence 20 (10) (1998) 1091–1096.

[54] Y. I. Abdel-Aziz, H. M. Karara, Direct linear transformation from comparator coordinates into object space coordinates in close-range photogrammetry, in: Proc. ASP/UI Symp. Close-Range Photogrammetry, Urbana, IL, 1971, pp. 1–18.